Attitude Dynamics Fundamentals

Hanspeter Schaub

Simulated Reprint from

Encyclopedia of Aerospace Engineering

Chichester, UK, 2010, pp. 3181–3198

Article Number: eae295

Section 5.5.1
Attitude Dynamics Fundamentals

Hanspeter Schaub

Aerospace Engineering Science Department, 431 UCB, University of Colorado, Boulder, CO 80309-0431, USA

Phone: (303) 492-2767 Fax: (303) 492-2825 Email: hanspeter.schaub@colorado.edu

File Name: attitude-fundamental.tex Software: LaTeX

Edited on: February 9, 2010

The rotational motion of a rigid body or system of rigid bodies is a fundamental field for the study of spacecraft pointing problems. This Chapter presents the fundamental aspects of describing the orientation, angular momentum, energy and differential equations of motion of a rigid body. After discussing the rigid body kinematics, the inertia properties of a body about arbitrary reference points are developed. The angular momentum and energy of a rigid body are critical to discussing the equations of motion, as well as investigating the stability of torque-free spin solutions. Next, passive methods of attitude stabilization are discussed. Here the spacecraft angular momentum, or external torques such as the gravity gradient torque, are used to stabilize the orientation. These fundamental kinematics and kinetics properties form the foundation for follow-on Chapters discussing more complex pointing scenarios including systems with multiple rigid bodies (reaction wheels, etc.), attitude estimation, as well active attitude pointing problems.

Keywords: *Rigid body pointing, angular momentum, rotational equations of motion, dual-spin spacecraft, gravity gradient torques*

1 RIGID BODY KINEMATICS

This Chapter first discusses the angular rotation and orientation coordinates used to describe the motion of a rigid body. By fixing a coordinate frame to a rigid body, understanding how the coordinate frame orientation evolves over time is equivalent to understanding how the rigid body attitude behaves.

1.1 Rotating Coordinate Frames

The coordinate frame $\mathcal{B} : \{\mathcal{O}, \hat{\boldsymbol{b}}_1, \hat{\boldsymbol{b}}_2, \hat{\boldsymbol{b}}_3\}$ illustrated in Figure 1 is defined through its origin $\mathcal{O}$ and the three mutually orthogonal unit direction vectors $\{\hat{\boldsymbol{b}}_1, \hat{\boldsymbol{b}}_2, \hat{\boldsymbol{b}}_3\}$. A right-handed coordinate frame satisfies $\hat{\boldsymbol{b}}_1 \times \boldsymbol{b}_2 = \hat{\boldsymbol{b}}_3$. If this coordinate frame $\mathcal{B}$ is attached to a rigid body, then describing the orientation of the rigid body is equivalent to studying the orientation of $\mathcal{B}$. For the study of attitude dynamics, the translation of the rigid body is not of interest. As a result

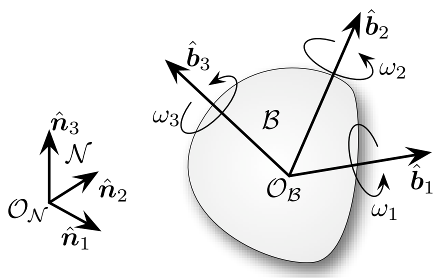

Figure 1: Coordinate Frame Illustration

coordinate frames are thus often defined through their unit direction vectors only.

As with positions, orientations can only be described relative to a reference orientation. Let $\mathcal{N}$ be an inertial (non-accelerating) coordinate frame. By defining the $\hat{\boldsymbol{b}}_i$ direction vectors with respect to $\mathcal{N}$, we are able to describe the orientation of the body $\mathcal{B}$ with respect to $\mathcal{N}$.

The angular motion of $\mathcal{B}$ relative to $\mathcal{N}$ is described through the angular velocity vector $\boldsymbol{\omega}_{\mathcal{B}/\mathcal{N}}$

$$\boldsymbol{\omega}_{\mathcal{B}/\mathcal{N}} = \omega_1 \hat{\boldsymbol{b}}_1 + \omega_2 \hat{\boldsymbol{b}}_2 + \omega_3 \hat{\boldsymbol{b}}_3 \tag{1}$$

This vector is the instantaneous angular rotation vector of body $\mathcal{B}$ relative to $\mathcal{N}$, and is typically expressed in body frame vector components. If only the $\mathcal{B}$ and $\mathcal{N}$ frames are considered, the $\boldsymbol{\omega}_{\mathcal{B}/\mathcal{N}}$ vector is often written simply as $\boldsymbol{\omega}$.

While we will see that attitude coordinates sets are not vectors, and do not abide by vector addition laws, amazingly the angular velocity vector is truly a vector. Thus, if three frames $\mathcal{A}$, $\mathcal{B}$ and $\mathcal{N}$ are present, their angular velocities relate through

$$\boldsymbol{\omega}_{\mathcal{A}/\mathcal{N}} = \boldsymbol{\omega}_{\mathcal{A}/\mathcal{B}} + \boldsymbol{\omega}_{\mathcal{B}/\mathcal{N}} \tag{2}$$

If we wish to express a vector $\boldsymbol{\omega}$ as a 3×1 matrix, we must specify with respect to which frame the vector components have been taken. If $\mathcal{B}$ frame components are used as in Eq. (1), then the left super-script notation is used in this Chapter:

$$^{\mathcal{B}}\boldsymbol{\omega} = {}^{\mathcal{B}}\!\begin{pmatrix} \omega_1 \\ \omega_2 \\ \omega_3 \end{pmatrix} \tag{3}$$

These frame declarations can become cumbersome after a while if only 2 frames are present. If no label is made on a matrix representation of a vector, then body frame components are implied.

Having defined a rotating frame $\mathcal{B}$, let us briefly discuss how to differentiate a vector $\boldsymbol{r}$ expressed in $\mathcal{B}$ vector components. To discuss the time evolution of $\boldsymbol{r}$, an observer frame must be specified. For example, if $\boldsymbol{r}$ points from the Space Shuttle cockpit to tail, then this vector appears stationary as seen by a Shuttle fixed observer. However, this same $\boldsymbol{r}$ is rotating as seen by an earth-fixed observer. A left super-script label is used on the time differential operator to denote the observer frame. The transport theorem is used to map a time derivative seen by a frame $\mathcal{B}$ into the equivalent derivative seen by another frame $\mathcal{N}$[Likins, 1973, Schaub and Junkins, 2010]:

$$\frac{^{\mathcal{N}}\mathrm{d}}{\mathrm{d}t}(\boldsymbol{r}) = \frac{^{\mathcal{B}}\mathrm{d}}{\mathrm{d}t}(\boldsymbol{r}) + \boldsymbol{\omega}_{\mathcal{B}/\mathcal{N}} \times \boldsymbol{r} \tag{4}$$

The vector $\boldsymbol{r}$ and frames $\mathcal{B}$ and $\mathcal{N}$ are only placeholders in Eq. (4). The transport theorem applies equally if any other vector or frames are substituted into this expression.

If no frame label is provided, then the time derivative is assumed to be taken with respect to an inertial frame.

$$\dot{\boldsymbol{x}} \equiv \frac{^{\mathcal{N}}\mathrm{d}}{\mathrm{d}t}(\boldsymbol{x}) \tag{5}$$

This is by far the most common time derivative of a vector as Newton's and Euler's laws require inertial derivatives to be taken. Further, let $\boldsymbol{x}$ be expressed in $\mathcal{B}$ frame components as $^{\mathcal{B}}\boldsymbol{x} = (x_1, x_2, x_3)^T$ Notice that

$$^{\mathcal{B}}\!\begin{pmatrix} \dot{x}_1 \\ \dot{x}_2 \\ \dot{x}_3 \end{pmatrix} \Rightarrow \frac{^{\mathcal{B}}\mathrm{d}}{\mathrm{d}t}(\boldsymbol{x}) \quad \not\Rightarrow \quad \dot{\boldsymbol{x}} \tag{6}$$

The time derivative of the angular velocity vector $\boldsymbol{\omega}_{\mathcal{B}/\mathcal{N}}$ has a special property worth noting:

$$\dot{\boldsymbol{\omega}}_{\mathcal{B}/\mathcal{N}} = \frac{^{\mathcal{B}}\mathrm{d}}{\mathrm{d}t}(\boldsymbol{\omega}_{\mathcal{B}/\mathcal{N}}) + \boldsymbol{\omega}_{\mathcal{B}/\mathcal{N}} \times \boldsymbol{\omega}_{\mathcal{B}/\mathcal{N}} = \frac{^{\mathcal{B}}\mathrm{d}}{\mathrm{d}t}(\boldsymbol{\omega}_{\mathcal{B}/\mathcal{N}}) \tag{7}$$

In other words, if $\boldsymbol{\omega}$ is the angular velocity vector between two particular frames, then the time derivative of $\boldsymbol{\omega}$ as seen by either of these frames is the same.

1.2 Attitude Parameters

Having shown how a rigid body rotation can be described through $\boldsymbol{\omega}$, these next sections focus on how the rigid body orientation is described. To describe the three-dimensional orientation of rigid body a minimum of three coordinates or attitude parameters are required. However, any minimal three-parameter set will encounter singularities that must be considered, while redundant sets of more than three parameters can avoid singularity issues at the cost of additional parameter constraints.

1.2.1 Direction Cosine Matrix

The 3×3 rotation matrix $[BN]$ is a fundamental way to express the orientation of $\mathcal{B}$ with respect to $\mathcal{N}$. Besides this 2-letter notation, $T_{\mathcal{B}}^{\mathcal{N}}$ is also used to represent the same matrix, or $[C]$ is often used if only a single body frame is considered. The rotation matrix is determined through

$$[BN] = \begin{bmatrix} \hat{\boldsymbol{b}}_1 \cdot \hat{\boldsymbol{n}}_1 & \hat{\boldsymbol{b}}_1 \cdot \hat{\boldsymbol{n}}_2 & \hat{\boldsymbol{b}}_1 \cdot \hat{\boldsymbol{n}}_3 \\ \hat{\boldsymbol{b}}_2 \cdot \hat{\boldsymbol{n}}_1 & \hat{\boldsymbol{b}}_2 \cdot \hat{\boldsymbol{n}}_2 & \hat{\boldsymbol{b}}_2 \cdot \hat{\boldsymbol{n}}_3 \\ \hat{\boldsymbol{b}}_3 \cdot \hat{\boldsymbol{n}}_1 & \hat{\boldsymbol{b}}_3 \cdot \hat{\boldsymbol{n}}_2 & \hat{\boldsymbol{b}}_3 \cdot \hat{\boldsymbol{n}}_3 \end{bmatrix} \tag{8}$$

Let α_{ij} be the angle between $\hat{\boldsymbol{b}}_i$ and $\hat{\boldsymbol{n}}_j$, then $\hat{\boldsymbol{b}}_i \cdot \hat{\boldsymbol{n}}_j = \cos\alpha_{ij}$. The rotation matrix elements BN_{ij} are thus the cosines of the relative unit direction angles. As a result the rotation matrix is also referred to as the Direction Cosine Matrix (DCM).

If the unit direction vectors $\hat{\boldsymbol{b}}_i$ are given in $\mathcal{N}$ frame components, or the unit direction vectors $\hat{\boldsymbol{n}}_i$ are expressed in $\mathcal{B}$ frame components, then the DCM is found through

$$[BN] = \begin{bmatrix} ({}^{\mathcal{N}}\hat{\boldsymbol{b}}_1)^T \\ ({}^{\mathcal{N}}\hat{\boldsymbol{b}}_2)^T \\ ({}^{\mathcal{N}}\hat{\boldsymbol{b}}_3)^T \end{bmatrix} = \begin{bmatrix} {}^{\mathcal{B}}\hat{\boldsymbol{n}}_1 & {}^{\mathcal{B}}\hat{\boldsymbol{n}}_2 & {}^{\mathcal{B}}\hat{\boldsymbol{n}}_3 \end{bmatrix} \tag{9}$$

The proper DCM (frame satisfy the right-hand rule) is orthogonal and has a determinant of +1. The inverse is simply given by the transpose operator:

$$[BN]^{-1} = [BN]^T = [NB] \tag{10}$$

The time evolution of the DCM orientation measure is captured through the differential kinematic equation

$$[\dot{BN}] = -[\tilde{\boldsymbol{\omega}}_{\mathcal{B}/\mathcal{N}}][BN] \tag{11}$$

where the tilde matrix notation is

$$[\tilde{\boldsymbol{\omega}}_{\mathcal{B}/\mathcal{N}}] = \begin{bmatrix} 0 & -\omega_3 & \omega_2 \\ \omega_3 & 0 & -\omega_1 \\ -\omega_2 & \omega_1 & 0 \end{bmatrix} \tag{12}$$

and represents a matrix representation of the vector cross product through $[\tilde{\omega}]\boldsymbol{a} \equiv \boldsymbol{\omega} \times \boldsymbol{a}$.

Assume that the DCMs $[AB]$ and $[BN]$ are given. To add these 2 orientations (sequentially rotate first from $\mathcal{N}$ to $\mathcal{B}$, and then rotate from $\mathcal{B}$ to $\mathcal{A}$), and obtain the attitude of $\mathcal{A}$ relative to $\mathcal{N}$, we simply multiply these DCM with each other:

$$[AN] = [AB][BN] \tag{13}$$

This simple DCM attitude addition property is a very fundamental method to add successive orientations. To subtract $[BN]$ from $[AN]$, and get the relative attitude of $\mathcal{A}$ relative to $\mathcal{B}$, we use

$$[AB] = [AN][BN]^{-1} = [AN][BN]^T = [AN][NB] \tag{14}$$

A common use of the DCM is to perform three-dimensional coordinate transformations. Assume a vector $\boldsymbol{r}$ is given in terms of $\mathcal{B}$ frame coordinates as

$$\boldsymbol{r} = r_1\hat{\boldsymbol{b}}_1 + r_2\hat{\boldsymbol{b}}_2 + r_3\hat{\boldsymbol{b}}_3 \tag{15}$$

To map ${}^{\mathcal{B}}\boldsymbol{r}$ into equivalent $\mathcal{N}$ vector components, the $[NB]$ rotation matrix is used:

$${}^{\mathcal{N}}\boldsymbol{r} = [NB]\,{}^{\mathcal{B}}\boldsymbol{r} \tag{16}$$

The inverse coordinate transformation is

$${}^{\mathcal{B}}\boldsymbol{r} = [NB]^{-1}\,{}^{\mathcal{N}}\boldsymbol{r} = [NB]^T\,{}^{\mathcal{N}}\boldsymbol{r} = [BN]\,{}^{\mathcal{N}}\boldsymbol{r} \tag{17}$$

1.2.2 Euler Angles

Euler angles are a minimal set of three attitude coordinates. All minimal orientation description contain attitudes where the description or the associated differential kinematic equations become singular. The Euler angles describe the orientation of $\mathcal{B}$ relative to $\mathcal{N}$ through 3 sequential one-axis rotations. There are 12 different sets of Euler angles which differ through the sequence of one-axis rotations. The popular yaw ψ, pitch θ and roll ϕ angles are a $(3-2-1)$ Euler angle sequence as illustrated in Figure 2. The primed axis labels denote the intermediate axes of the rotation sequence. Starting with $\mathcal{N}$ frame orientation, the yaw axis is defined as positive rotation about the current 3-axis ($\hat{\boldsymbol{n}}_3$ or $\hat{\boldsymbol{b}}_3$), the pitch is a rotation about the current 2-axis ($\hat{\boldsymbol{b}}'_2$ or $\hat{\boldsymbol{b}}''_2$), and the roll is a rotation about the final 1-axis ($\hat{\boldsymbol{b}}''_1$ or $\hat{\boldsymbol{b}}_1$).

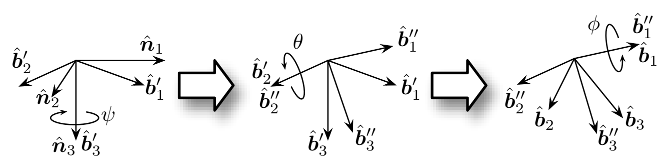

Figure 2: (3-2-1) Euler Angle Sequence

The one-dimensional rotations about the i^{th} body axis can be describe using rotation matrices $[M_i(\theta)]$ as:

$$[M_1(\theta)] = \begin{bmatrix} 1 & 0 & 0 \\ 0 & \cos\theta & \sin\theta \\ 0 & -\sin\theta & \cos\theta \end{bmatrix} \tag{18a}$$

$$[M_2(\theta)] = \begin{bmatrix} \cos\theta & 0 & -\sin\theta \\ 0 & 1 & 0 \\ \sin\theta & 0 & \cos\theta \end{bmatrix} \tag{18b}$$

$$[M_3(\theta)] = \begin{bmatrix} \cos\theta & \sin\theta & 0 \\ -\sin\theta & \cos\theta & 0 \\ 0 & 0 & 1 \end{bmatrix} \tag{18c}$$

Using the DCM addition property in Eq. (13), the (3-2-1) yaw, pitch and roll rotations lead to

$$[BN] = [M_1(\phi)][M_2(\theta)][M_3(\psi)] \tag{19}$$

or

$$[BN] = \begin{bmatrix} c\theta c\psi & c\theta s\psi & -s\theta \\ s\phi s\theta c\psi - c\phi s\psi & s\phi s\theta s\psi + c\phi c\psi & s\phi c\theta \\ c\phi s\theta c\psi + s\phi s\psi & c\phi s\theta s\psi - s\phi c\psi & c\phi c\theta \end{bmatrix} \tag{20}$$

The inverse transformations from the direction cosine matrix $[BN]$ to the (ψ, θ, ϕ) angles are

$$\psi = \arctan\left(\frac{BN_{12}}{BN_{11}}\right) \tag{21a}$$

$$\theta = -\arcsin\left(BN_{13}\right) \tag{21b}$$

$$\phi = \arctan\left(\frac{BN_{23}}{BN_{33}}\right) \tag{21c}$$

A good description of alternate sets of Euler angles can be found in Junkins and Turner [1986].

To add or subtract two orientations given in terms of Euler angles, these angles are mapped to the equivalent DCM (using Eq. (19) for the (3-2-1) Euler angles) and then using the simple DCM attitude addition and subtraction properties in Eqs. (13) and (14). Having obtained the desired DCM, the equivalent $(3-2-1)$ Euler angles can be extracted using Eq. 21.

The differential kinematic equations relate the (3-2-1) Euler angle rates to the body angular velocity vector $\boldsymbol{\omega}$ through[Shuster, 1993]

$$\begin{pmatrix} \dot{\psi} \\ \dot{\theta} \\ \dot{\phi} \end{pmatrix} = \underbrace{\begin{bmatrix} 0 & \frac{\sin\phi}{\cos\theta} & \frac{\cos\phi}{\cos\theta} \\ 0 & \cos\phi & -\sin\phi \\ 1 & \sin\phi\tan\theta & \cos\phi\tan\theta \end{bmatrix}}_{[B(\psi,\theta,\phi)]} {}^{\mathcal{B}}\!\begin{pmatrix} \omega_1 \\ \omega_2 \\ \omega_3 \end{pmatrix} \tag{22}$$

Note that the $\boldsymbol{\omega}$ vector components here must be taken with respect to the $\mathcal{B}$ frame because the Euler angles define the attitude of $\mathcal{B}$. Further, these kinematic differential equations are singular if the 2nd rotation angle θ is ± 90 degrees. This singular behavior is true for all Euler angle sequences which do not repeat a rotation axis (asymmetric Euler angles). If a rotation axis is repeated such as a (3-1-3) sequence, then the attitude coordinates are called symmetric Euler angles. In this case it is also the 2nd rotation angle θ_2 which determines a singular orientation, but it must be $\theta_2 = 0$ or 180 degrees.

Besides the (3-2-1) yaw, pitch and roll Euler angles, the (3-1-3) Euler angles are also popular to describe spacecraft or orbit plane orientations. The DCM in terms of (3-1-3) Euler angles (Ω, i, ω) is

$$[BN] = \begin{bmatrix} c\omega c\Omega - s\omega cis\Omega & s\omega cic\Omega + c\omega s\Omega & s\omega si \\ -s\omega c\Omega - c\omega cis\Omega & c\omega cic\Omega - s\omega s\Omega & c\omega si \\ sis\Omega & -sic\Omega & ci \end{bmatrix} \tag{23}$$

while the differential kinematic equation is

$$\begin{pmatrix} \dot{\Omega} \\ \dot{i} \\ \dot{\omega} \end{pmatrix} = \underbrace{\begin{bmatrix} \frac{\sin\omega}{\sin i} & \frac{\cos\omega}{\sin i} & 0 \\ \cos\omega & -\sin\omega & 0 \\ -\sin\omega\cot i & -\cos\omega\cot i & 1 \end{bmatrix}}_{[B(\Omega,i,\omega)]} {}^{\mathcal{B}}\!\begin{pmatrix} \omega_1 \\ \omega_2 \\ \omega_3 \end{pmatrix} \tag{24}$$

1.2.3 *Principal Rotation Parameters*

While the Euler angles utilize three sequencial rotations to map from $\mathcal{N}$ to $\mathcal{B}$, it is possible to rotate between two arbitrary frame using a single rotation about the principal axis $\hat{\boldsymbol{e}}$ by the principal angle Φ. This property is called Euler's Principle Rotation theorem.[Whittaker, 1965 reprint] The principal rotation axis $\hat{\boldsymbol{e}}$ has the special property that

$${}^{\mathcal{B}}\hat{\boldsymbol{e}} = [BN]\, {}^{\mathcal{N}}\hat{\boldsymbol{e}} \tag{25}$$

Thus $\hat{\boldsymbol{e}}$ is the eigenvector of $[BN]$ corresponding to the +1 eigenvalue.

The principal rotation parameters $\hat{\boldsymbol{e}}$ and Φ are not unique. An orientation can be represented through

$$(\hat{\boldsymbol{e}}, \Phi) \qquad (-\hat{\boldsymbol{e}}, -\Phi) \qquad (\hat{\boldsymbol{e}}, \Phi') \qquad (-\hat{\boldsymbol{e}}, -\Phi') \tag{26}$$

where $\Phi' = 2\pi - \Phi$. While one principal angle Φ describes the short rotation, say 30 degrees, the alternate principal angle Φ' describes the long rotation representation, say 330 degrees.

The DCM in terms of $(\hat{e}, \Phi)$ is given by[Shuster, 1993]

$$[BN] = \cos\Phi[I_{3\times3}] + (1 - \cos\Phi)\, \hat{\boldsymbol{e}}\hat{\boldsymbol{e}}^T - \sin\Phi[\tilde{\boldsymbol{e}}] \tag{27}$$

The inverse transformation from the rotation matrix $[BN]$ to the principal rotation parameters is

$$\Phi = \pm\arccos\left(\frac{1}{2}\left(\text{trace}([BN]) - 1\right)\right) \tag{28a}$$

$$\hat{\boldsymbol{e}} = \frac{1}{2\sin\Phi}\begin{pmatrix} BN_{23} - BN_{32} \\ BN_{31} - BN_{13} \\ BN_{12} - BN_{21} \end{pmatrix} \tag{28b}$$

The four different principal rotation parameter sets are obtained by using either sign in Eq. (28a) and noting the alternate $\Phi' = 2\pi - \Phi$ solution to the $\arccos$ function.

1.2.4 *Quaternions or Euler Parameters*

The quaternions, also called the Euler Parameters (EPs), are a popular redundant attitude coordinate set which is singularity free in its attitude representation. The Euler parameter set $\boldsymbol{\beta} = (\beta_0, \beta_1, \beta_2, \beta_3)$ is defined in terms of the principal rotation parameters as

$$\beta_0 = \cos\left(\Phi/2\right) \tag{29a}$$

$$\beta_1 = e_1 \sin\left(\Phi/2\right) \tag{29b}$$

$$\beta_2 = e_2 \sin\left(\Phi/2\right) \tag{29c}$$

$$\beta_3 = e_3 \sin\left(\Phi/2\right) \tag{29d}$$

Note that β_0 only depends on the principal rotation angle, and is not influenced by the principal rotation axis, and is thus called the scalar EP component. The remaining EP β_1, β_2 and β_3 are referred to as the vector EP components. Alternate variable notations such as (q_1, q_2, q_3, q_4) are also popular. Care should be taken how the scalar EP or quaternion component is labeled ($q_4 = \beta_0$ in this case).

Being a redundant 4-parameter set, the EPs must satisfy the holonomic constraint

$$\beta_0^2 + \beta_1^2 + \beta_2^2 + \beta_3^2 = 1 \tag{30}$$

If numerically integrating the EPs, this constraint must be enforced at each time step. As we had 4 sets of possible principal rotation parameters to represent an orientation, this results in 2 sets of feasible EPs $\boldsymbol{\beta}$ and $\boldsymbol{\beta}' = -\boldsymbol{\beta}$. If β_0 of an EP set is greater than zero, then the EPs are describing a short rotation from $\mathcal{N}$ to $\mathcal{B}$ with Φ <180 degrees. If $\beta_0 < 0$ then a long rotation is described. This duality is important when choosing which set of EPs is used in a feedback attitude control problem.

The DCM is written in terms of the EPs as

$$[BN] = \begin{bmatrix} \beta_0^2+\beta_1^2-\beta_2^2-\beta_3^2 & 2(\beta_1\beta_2+\beta_0\beta_3) & 2(\beta_1\beta_3-\beta_0\beta_2) \\ 2(\beta_1\beta_2-\beta_0\beta_3) & \beta_0^2-\beta_1^2+\beta_2^2-\beta_3^2 & 2(\beta_2\beta_3+\beta_0\beta_1) \\ 2(\beta_1\beta_3+\beta_0\beta_2) & 2(\beta_2\beta_3-\beta_0\beta_1) & \beta_0^2-\beta_1^2-\beta_2^2+\beta_3^2 \end{bmatrix} \tag{31}$$

while the inverse mapping is

$$\beta_0 = \pm\frac{1}{2}\sqrt{\text{trace}([BN])+1} \tag{32a}$$

$$\beta_1 = \frac{BN_{23} - BN_{32}}{4\beta_0} \tag{32b}$$

$$\beta_2 = \frac{BN_{31} - BN_{13}}{4\beta_0} \tag{32c}$$

$$\beta_3 = \frac{BN_{12} - BN_{21}}{4\beta_0} \tag{32d}$$

As expected, this mapping yields 2 possible EP sets. Note that this algorithm in singular if β_0 = 0 (Φ = 180 degrees). A lengthier, but singularity free, mapping from DCM into equivalent EPs is given by Sheppard [1978].

To add or subtract EP sets it is not necessary to map the EPs to and from DCMs. Instead the EP have a direct bilinear transformation. Let $\boldsymbol{\beta}'$ and $\boldsymbol{\beta}''$ represent to orientations which are to be added to yield the overall rotation as the EP set $\boldsymbol{\beta}$.

$$\begin{pmatrix}\beta_0\\\beta_1\\\beta_2\\\beta_3\end{pmatrix} = \begin{bmatrix} \beta_0'' & -\beta_1'' & -\beta_2'' & -\beta_3'' \\ \beta_1'' & \beta_0'' & \beta_3'' & -\beta_2'' \\ \beta_2'' & -\beta_3'' & \beta_0'' & \beta_1'' \\ \beta_3'' & \beta_2'' & -\beta_1'' & \beta_0'' \end{bmatrix} \begin{pmatrix}\beta_0'\\\beta_1'\\\beta_2'\\\beta_3'\end{pmatrix} \tag{33}$$

By *transmutation* of Eq. (33) an alternate $\boldsymbol{\beta}$ expression is found

$$\begin{pmatrix}\beta_0\\\beta_1\\\beta_2\\\beta_3\end{pmatrix} = \begin{bmatrix} \beta_0' & -\beta_1' & -\beta_2' & -\beta_3' \\ \beta_1' & \beta_0' & -\beta_3' & \beta_2' \\ \beta_2' & \beta_3' & \beta_0' & -\beta_1' \\ \beta_3' & -\beta_2' & \beta_1' & \beta_0' \end{bmatrix} \begin{pmatrix}\beta_0''\\\beta_1''\\\beta_2''\\\beta_3''\end{pmatrix} \tag{34}$$

The 4×4 matrices in Eqs. (33) and (34) are orthogonal with their inverse simply being the transpose of the matrix. This makes it straight-forward to subtract two orientations and solve for the relative orientation $\boldsymbol{\beta}'$ given $\boldsymbol{\beta}$ and $\boldsymbol{\beta}''$ using Eq. (33).

The EP rates relate to the body angular velocity vector $\boldsymbol{\omega}$ through

$$\begin{pmatrix}\dot\beta_0\\\dot\beta_1\\\dot\beta_2\\\dot\beta_3\end{pmatrix} = \frac{1}{2}\begin{bmatrix} 0 & -\omega_1 & -\omega_2 & -\omega_3 \\ \omega_1 & 0 & \omega_3 & -\omega_2 \\ \omega_2 & -\omega_3 & 0 & \omega_1 \\ \omega_3 & \omega_2 & -\omega_1 & 0 \end{bmatrix} \begin{pmatrix}\beta_0\\\beta_1\\\beta_2\\\beta_3\end{pmatrix} \tag{35}$$

or by transmutation

$$\begin{pmatrix}\dot\beta_0\\\dot\beta_1\\\dot\beta_2\\\dot\beta_3\end{pmatrix} = \frac{1}{2}\begin{bmatrix} \beta_0 & -\beta_1 & -\beta_2 & -\beta_3 \\ \beta_1 & \beta_0 & -\beta_3 & \beta_2 \\ \beta_2 & \beta_3 & \beta_0 & -\beta_1 \\ \beta_3 & -\beta_2 & \beta_1 & \beta_0 \end{bmatrix} \begin{pmatrix}0\\\omega_1\\\omega_2\\\omega_3\end{pmatrix} \tag{36}$$

The 4×4 matrix in Eq. (36) is again orthogonal and enjoys a simple inverse formulation.

1.2.5 Other Attitude Parameters

There are several other sets of attitude parameters such as the (w, z) coordinates introduced by Tsiotras and Longuski [1996], or the Calyey-Klein parameters discussed by Whittaker [1965 reprint]. A good survey of attitude coordinates is published by Shuster [1993]. Besides using the quaternions as a singularity free attitude measure, the Modified Rodrigues Parameters (MRPs) have become popular.[Wiener, 1962] At the cost of a discontinuous attitude description, the MRPs can represent any orientation without singularity using only 3 parameters.[Schaub and Junkins, 1996]

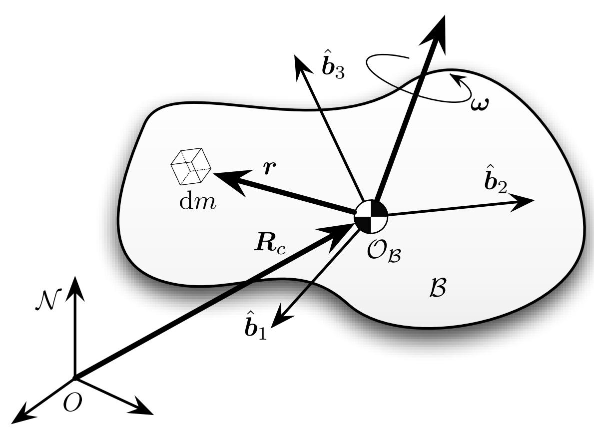

Figure 3: Discretized Continuous Body

2 RIGID BODY INERTIA

Having covered how to describe the orientation of a rigid body (kinematics), we now focus on how bodies with specific mass distributions will rotate (kinetics). This leads to the basic rotational equations of motion dictating how a rigid body will accelerate rotationally due to external torques.

2.1 Inertia Matrix Definition

Assume a rigid body has a body-fixed coordinate frame $\mathcal{B}$ as illustrated in Figure 3. The origin $\mathcal{O}_\mathcal{B}$ is set to be equal to the center of mass location of the rigid body. Let $\boldsymbol{r}$ be the position vector of a differential mass element $\mathrm{d}m$. The 3×3 inertia matrix of this rigid body about its center of mass point is defined as [Schaub and Junkins, 2010]

$$[I_c] = \int_B -[\tilde{\boldsymbol{r}}][\tilde{\boldsymbol{r}}]\mathrm{d}m \tag{37}$$

where $\int_\mathcal{B}$ represents the integral over the entire body $\mathcal{B}$. If $\boldsymbol{r}$ is expressed in $\mathcal{B}$ frame components as in Eq. (15), then the symmetric inertia matrix is expressed in $\mathcal{B}$ frame component form as

$${}^\mathcal{B}[I_c] = \int_B {}^\mathcal{B}\begin{bmatrix} r_2^2 + r_3^2 & -r_1 r_2 & -r_1 r_3 \\ -r_1 r_2 & r_1^2 + r_3^2 & -r_2 r_3 \\ -r_1 r_3 & -r_2 r_3 & r_1^2 + r_2^2 \end{bmatrix} \mathrm{d}m \tag{38}$$

If the body contains a series of discrete mass elements, then the integral in Eq. (38) can also be replaced with a summation operator.

2.2 Principal Coordinate System

Note that the inertia matrix calculation in Eq. (37) depends on the choice of the body frame $\mathcal{B}$ used to represent $\boldsymbol{r}$. What if the inertia matrix is required with respect to another body fixed frame $\mathcal{F}$? Fortunately there exists a direct transformation of ${}^\mathcal{B}[I_c]$ into ${}^\mathcal{F}[I_c]$ that maps one inertia matrix to any other frame without performing the body integral again. Let $[FB]$ be the DCM of the new body-fixed frame $\mathcal{F}$ relative to the previous body frame $\mathcal{B}$. The inertia matrix coordinate frame transformation is then given by [Schaub and Junkins, 2010]

$${}^\mathcal{F}[I] = [FB]\,{}^\mathcal{B}[I]\,[FB]^T \tag{39}$$

Generally the $[I_c]$ matrix is a fully populated 3×3 matrix. Studying Eq. (39) raises the following question. Is it possible to pick $\mathcal{F}$ such that the resulting inertia matrix ${}^\mathcal{F}[I]$ is diagonal with

$${}^\mathcal{F}[I] = {}^\mathcal{F}\begin{bmatrix} I_1 & 0 & 0 \\ 0 & I_2 & 0 \\ 0 & 0 & I_3 \end{bmatrix} \tag{40}$$

The answer, naturally, is yes. Let $\boldsymbol{v}_i$ be unit eigenvectors of the inertia matrix ${}^\mathcal{B}[I]$ and λ_i be the corresponding eigenvalues. The desired coordinate transformation matrix $[FB]$ is

$$[FB] = \begin{bmatrix} \boldsymbol{v}_1^T \\ \boldsymbol{v}_2^T \\ \boldsymbol{v}_3^T \end{bmatrix} \tag{41}$$

Note that because the order, magnitude and sign of the eigenvectors $\boldsymbol{v}_i$ is not unique, the $[FB]$ rotation is also not unique. The $\mathcal{F}$ frame unit direction vectors $\hat{\boldsymbol{f}}_i$ are then given by

$${}^\mathcal{B}\hat{\boldsymbol{f}}_1 = \boldsymbol{v}_1 \qquad {}^\mathcal{B}\hat{\boldsymbol{f}}_2 = \boldsymbol{v}_2 \qquad {}^\mathcal{B}\hat{\boldsymbol{f}}_3 = {}^\mathcal{B}\hat{\boldsymbol{f}}_1 \times {}^\mathcal{B}\hat{\boldsymbol{f}}_2 \tag{42}$$

Determining ${}^\mathcal{B}\hat{\boldsymbol{f}}_3$ in this manner guarantees that $\mathcal{F}$ ends up as a proper right-handed coordinate system. The $\mathcal{F}$ frame axes $\hat{\boldsymbol{f}}_i$ which diagonalize the rigid body inertia matrix are called the *principal axes*. The frame $\mathcal{F}$ then is a *principal coordinate frame* of the body, with the eigenvalues λ_i being the *principal inertias* I_i of this body.

For example, consider the inertia matrix expression with respect to a general body-fixed frame $\mathcal{B}$:

$${}^\mathcal{B}[I] = {}^\mathcal{B}\begin{bmatrix} 28.700 & -2.279 & 2.340 \\ -2.279 & 24.400 & 1.585 \\ 2.340 & 1.585 & 21.900 \end{bmatrix} \text{kg} \cdot \text{m}^2 \tag{43}$$

The principal inertias of this body are determined through the eigenvalues $(30, 25, 20)$ kg·m^2. The corresponding eigenvectors are

$$\boldsymbol{v}_1 = {}^\mathcal{B}\begin{bmatrix} 0.925 \\ -0.319 \\ 0.205 \end{bmatrix} \quad \boldsymbol{v}_2 = {}^\mathcal{B}\begin{bmatrix} 0.163 \\ 0.823 \\ 0.544 \end{bmatrix} \quad \boldsymbol{v}_3 = {}^\mathcal{B}\begin{bmatrix} -0.342 \\ -0.470 \\ 0.814 \end{bmatrix} \tag{44}$$

The desired rotation matrix $[FB]$ to rotate the general body frame $\mathcal{B}$ into a principal coordinate frame is

$$[FB] = \begin{bmatrix} 0.925 & -0.319 & 0.205 \\ 0.163 & 0.823 & 0.544 \\ -0.342 & -0.470 & 0.814 \end{bmatrix} \tag{45}$$

Here the eigenvector algorithm returned a set of vectors $\boldsymbol{v}_i$ where $\boldsymbol{v}_1 \times \boldsymbol{v}_2 = \boldsymbol{v}_3$. This is generally not the case and this condition must be checked.

2.3 Parallel Axis Theorem

If the inertia matrix is not required about the body center of mass, but about another point O, then we would like to do this computation without reevaluating the body intergral in Eq. (37). Let $\boldsymbol{R}_c$ be the position vector from the point O to the body center of mass. The *parallel axis theorem* is used to map $[I_c]$ into the body inertia matrix $[I_O]$ taken about O using [Schaub and Junkins, 2010]

$$[I_O] = [I_c] + M[\tilde{\boldsymbol{R}}_c][\tilde{\boldsymbol{R}}_c]^T \tag{46}$$

Note that this equation is written in a coordinate frame independent manner. When evaluating the numerical values of the inertias, care must be taken that both $[I_c]$ and $\boldsymbol{R}_c$ are expressed with respect to the same coordinate frames. If not, the DCM is used to rotate either the inertia matrix components (see Eq. (39)) or the position vectors components (see Eq. (16)) into the appropriate frame.

Let us consider the following example. The inertia of a body about its center of mass is given in Eq. (43). The body is placed inside the space shuttle bay. The body mass is $M = 20$ kg. Let $\mathcal{S} : \{\hat{\boldsymbol{s}}_1, \hat{\boldsymbol{s}}_2, \hat{\boldsymbol{s}}_3\}$ be the space-shuttle fixed frame, and

$$\boldsymbol{r}_{\mathcal{B}/\mathcal{S}} = (1\text{ m})\hat{\boldsymbol{s}}_1 + (2\text{ m})\hat{\boldsymbol{s}}_2 - (1\text{ m})\hat{\boldsymbol{s}}_3 \tag{47}$$

We wish to evaluate the the inertia the body $\mathcal{B}$ about the origin of $\mathcal{S}$. Before we can use the parallel axis theorem, note that $[I]$ is given in $\mathcal{B}$ frame vector components, while $\boldsymbol{r}_{\mathcal{B}/\mathcal{S}}$ is given in terms of $\mathcal{S}$ frame components. Let the relative orientation of $\mathcal{B}$ with respect to $\mathcal{S}$ be

$$[BS] = \begin{bmatrix} 0 & 0 & -1 \\ -1 & 0 & 0 \\ 0 & 1 & 0 \end{bmatrix} \tag{48}$$

If the final expression is desired in shuttle $\mathcal{S}$-frame components, it is simplest to perform a coordinate transformation of the body inertia $[I]$ into $\mathcal{S}$-frame components using Eq. (39).

$$\begin{aligned} {}^{\mathcal{S}}[I] &= [BS]^T \, {}^{\mathcal{B}}[I] \, [BS] \\ &= {}^{\mathcal{S}}\begin{bmatrix} 24.40 & -1.59 & -2.28 \\ -1.59 & 21.90 & -2.34 \\ -2.28 & -2.24 & 28.70 \end{bmatrix} \text{kg} \cdot \text{m}^2 \end{aligned} \tag{49}$$

Now the desired inertia matrix of $\mathcal{B}$ about the origin O of $\mathcal{S}$ is evaluated using Eq. (46):

$$\begin{aligned} {}^{\mathcal{S}}[I_O] &= {}^{\mathcal{S}}[I] + M[\tilde{\boldsymbol{r}}_{\mathcal{B}/\mathcal{S}}][\tilde{\boldsymbol{r}}_{\mathcal{B}/\mathcal{S}}]^T \\ &= {}^{\mathcal{S}}\begin{bmatrix} 124.40 & -41.59 & -17.72 \\ -41.59 & 61.90 & 37.66 \\ 17.72 & 37.66 & 128.70 \end{bmatrix} \text{kg} \cdot \text{m}^2 \end{aligned} \tag{50}$$

3 ANGULAR MOMENTUM

The total angular momentum of the continuous body of mass M shown in Figure 3 is written as

$$\boldsymbol{H}_O = \boldsymbol{R}_c \times M\dot{\boldsymbol{R}}_c + \int_B \boldsymbol{r} \times \dot{\boldsymbol{r}} \mathrm{d}m \tag{51}$$

Here $\boldsymbol{R}_c \times M\dot{\boldsymbol{R}}_c$ is the angular momentum of the body center of mass about point O, while

$$\boldsymbol{H}_c = \int_B \boldsymbol{r} \times \dot{\boldsymbol{r}} \mathrm{d}m \tag{52}$$

is the angular momentum of the body about the center of mass. The vector $\boldsymbol{r}$ is the position of each differential mass element $\mathrm{d}m$ relative to the body center of mass. If the body is rigid, then $\dot{\boldsymbol{r}} = \boldsymbol{\omega} \times \boldsymbol{r}$ and

$$\boldsymbol{H}_c = \int_B \boldsymbol{r} \times (\boldsymbol{\omega} \times \boldsymbol{r}) \, \mathrm{d}m = [I_c]\boldsymbol{\omega} \tag{53}$$

where $[\tilde{\boldsymbol{a}}]\boldsymbol{b} \equiv \boldsymbol{a} \times \boldsymbol{b}$ and the inertia definition in Eq. (37) is used. To study the rotational motion of a rigid body about its center of mass we focus on $\boldsymbol{H}_c$ and do not consider the spacecraft translation as a whole. If a principal coordinate frame $\mathcal{B}$ is chosen, then $|\boldsymbol{H}_c|^2$ is written as

$$H^2 = |\boldsymbol{H}_c|^2 = I_1^2\omega_1^2 + I_2^2\omega_2^2 + I_3^2\omega_3^2 \tag{54}$$

Let $\boldsymbol{L}$ be the total external torque acting on the rigid body. This torque could be due to the spacecraft actuator thrusters, or be environment torques such as the gravity gradient, atmospheric, or differential solar radiation torque. Euler's equation states that

$$\dot{\boldsymbol{H}} = \boldsymbol{L} \tag{55}$$

This very simple and innocent looking differential equation is the means to compute the rotational equations of motion of a rigid body, or even a system of rigid bodies. Thus, let us discuss Eq. (55) in more detail. First, the time derivative of the $\boldsymbol{H}$ vector must be taken as seen by an inertial coordinate frame. Euler's equation is not only valid for a system containing a single rigid body, it is also valid for a system containing N rigid bodies. The angular momentum expression $\boldsymbol{H} = \sum_{i=1}^{N} \boldsymbol{H}_i$ must be the total angular momentum, where $\boldsymbol{H}_i$ could represent the momentum of the the spacecraft, a moving panel, or an attached fly-wheel. Finally, care must be taken in Eq. (55) both the momentum and the torque vectors are taken about the identical reference point. This hinge point can be an inertial point, or the system center of mass.

4 KINETIC ENERGY

Referring again to Figure 3, the kinetic energy of a rigid body is

$$T = \frac{1}{2}M\dot{\boldsymbol{R}}_c \cdot \dot{\boldsymbol{R}}_c + \frac{1}{2}\int_B \dot{\boldsymbol{r}} \cdot \dot{\boldsymbol{r}} \mathrm{d}m = T_{\text{trans}} + T_{\text{rot}} \tag{56}$$

For attitude studies we focus again on the rotational energy only, and ignore the translational motion of the body center of mass. Using $[\tilde{\boldsymbol{a}}]\boldsymbol{b} \equiv \boldsymbol{a} \times \boldsymbol{b}$ and the inertia definition in Eq. (37), the rotational energy of a single rigid body is [Curtis, 2010]

$$T_{\text{rot}} = \frac{1}{2}\int_B \dot{\boldsymbol{r}} \cdot \dot{\boldsymbol{r}} \mathrm{d}m = \frac{1}{2}\boldsymbol{\omega}^T[I_c]\boldsymbol{\omega} = \frac{1}{2}\boldsymbol{\omega} \cdot \boldsymbol{H}_c \tag{57}$$

If a principal coordinate system is chosen for $\mathcal{B}$, the energy is written using the principal inertias I_i as

$$T_{\text{rot}} = \frac{I_1}{2}\omega_1^2 + \frac{I_2}{2}\omega_2^2 + \frac{I_3}{2}\omega_3^2 \tag{58}$$

The power equation seeks to determine what the energy rate $\dot{T}$ is for a dynamical system. Let $\boldsymbol{L}_c$ be the total external torque acting on a rigid body about the body center of mass. This torque will cause the rotational energy to vary according to

$$\dot{T}_{\text{rot}} = \boldsymbol{\omega} \cdot \boldsymbol{L}_c \tag{59}$$

The derivation of this power equation requires use of the rigid body rotational equations of motion in Eq. (61). Note that even though T is computed using the vectors $\boldsymbol{\omega}$ and $\boldsymbol{H}_c$ in Eq. (57), the answer is a scalar. The time derivative of scalar quantities is the same no matter what observer frame is used. Thus, the power equations in Eq. (59) can be obtain by differentiating the vectors with respect to *any* frame.

5 ROTATIONAL EQUATIONS OF MOTION

5.1 Euler's Rotational Equations

Let us assume at first the the rigid body has a fully populated inertia matrix $[I]$. Note that in this development all moments and torques are implied to be taken about the body center of mass, and the subscript "c" is dropped for convenience. The rotational equations of motion are obtained by evaluating Euler's equation in Eq. (55) using the transport theorem in Eq. (4):

$$\begin{aligned}\dot{\boldsymbol{H}} &= \frac{{}^{\mathcal{B}}\mathrm{d}}{\mathrm{d}t}(\boldsymbol{H}) + \boldsymbol{\omega}\times\boldsymbol{H} = \boldsymbol{L}\\ &= \frac{{}^{\mathcal{B}}\mathrm{d}}{\mathrm{d}t}([I])\,\boldsymbol{\omega} + [I]\frac{{}^{\mathcal{B}}\mathrm{d}}{\mathrm{d}t}(\boldsymbol{\omega}) + [\tilde{\boldsymbol{\omega}}][I]\boldsymbol{\omega} = \boldsymbol{L}\end{aligned} \tag{60}$$

Because the body is rigid we find that $\frac{{}^{\mathcal{B}}\mathrm{d}}{\mathrm{d}t}([I])$ is zero. Using Eq. (7) the famous Euler's rotational equations of motion of a body with a general inertia matrix are found:

$$[I]\dot{\boldsymbol{\omega}} = -[\tilde{\omega}][I]\boldsymbol{\omega} + \boldsymbol{L} \tag{61}$$

Choosing a principal body fixed coordinate system the inertia matrix $[I]$ is diagonal and Eq. (61) reduces to [Wiesel, 1989]

$$I_{11}\dot{\omega}_1 = -(I_{33} - I_{22})\omega_2\omega_3 + L_1 \tag{62a}$$
$$I_{22}\dot{\omega}_2 = -(I_{11} - I_{33})\omega_3\omega_1 + L_2 \tag{62b}$$
$$I_{33}\dot{\omega}_3 = -(I_{22} - I_{11})\omega_1\omega_2 + L_3 \tag{62c}$$

Here L_i are the body frame $\mathcal{B}$ vector components of the external torque vector $\boldsymbol{L}$.

5.2 Principal Axis Spin Stability

Note that due to the gyroscopic cross coupling terms in Eq. (62), the only spin equilibria (where $\dot{\boldsymbol{\omega}} = 0$) of a rigid body occurs when a pure spin about a principal axis is performed.

$$\boldsymbol{\omega}_e = \omega_e \hat{\boldsymbol{b}}_i \qquad \text{for } i = 1, 2, 3 \tag{63}$$

Here two ω_i are zero initially resulting in zero $\dot{\boldsymbol{\omega}}$. These pure principal axis spin conditions are common with many spin-stabilized spacecraft. We next investigate the linear stability of such principal axis spins. Let $\mathcal{B}$ be a principal body-fixed frame. Without loss of generality assume the body is nominally spinning about $\hat{\boldsymbol{b}}_1$ with $\boldsymbol{\omega}_e = \omega_{e_1}\hat{\boldsymbol{b}}_1$ and that $\omega_{e_2} = \omega_{e_3} = 0$. Next we assume the spin experiences small departures through $\omega_i = \omega_{e_i} + \delta\omega_i$ and linearize the equations of motion in Eq. (62):

$$\delta\dot{\omega}_1 = 0 \tag{64a}$$
$$\delta\dot{\omega}_2 = \frac{I_3 - I_1}{I_2}\omega_{e_1}\delta\omega_3 \tag{64b}$$
$$\delta\dot{\omega}_3 = \frac{I_1 - I_2}{I_3}\omega_{e_1}\delta\omega_2 \tag{64c}$$

Immediately it is apparent that the spin departures $\delta\omega_1$ about the nominal spin axis are marginally stable. Given an initial spin error $\delta\omega_1(t_0)$ the spin is constant:

$$\omega_1(t) = \omega_{e_1} + \delta\omega_1(t_0) \tag{65}$$

The spin about the other two axis are coupled. Differentiating Eq. (64c), substituting into Eq. (64b), and simplifying yields the uncoupled result for $\delta\omega_2$.

$$\delta\ddot{\omega}_2 + \underbrace{\left(\frac{I_1 - I_3}{I_2}\omega_{e_1}\right)\left(\frac{I_1 - I_2}{I_3}\omega_{e_1}\right)}_{k}\delta\omega_2 = 0 \tag{66}$$

Similarly the $\delta\omega_3$ motion is shown to satisfy

$$\delta\ddot{\omega}_3 + k\delta\omega_3 = 0 \tag{67}$$

Thus, $k > 0$ for the spin about the equilibrium $\boldsymbol{\omega}_e = \omega_{e_1}\hat{\boldsymbol{b}}_1$ to be linearly stable. This is true if I_1 is either the largest or the smallest inertia. Any spin about the intermediate axis of inertia is guaranteed to be unstable. Note that the spin about the largest moment of inertia is always stable. However, as will be shown in the study of the polhodes, the spin about the least moment of inertia is only stable in the absence of energy dissipation.

5.3 Numerical Simulation of Rigid Body Motion

The rotational equations of motion in Eq. (61) appear at first glance to be decoupled from any attitude coordinates. However, the orientation can couple into these equations if the external torque $\boldsymbol{L}$ depends on the attitude. Such external torques include atmospheric torque, solar radiation torque, gravity gradient torques, etc. Writing a numerical integration routine for the spacecraft attitude, Euler's rotational equations of motion in Eq. (61) need to be integrated simulateneously with the appropriate kinematic differential equations such as Eq. (22) or Eq. (36).

6 TORQUE-FREE RESPONSE

The remainder of this section studies the rotational motion of a rigid body in the absence of an external torque vector. This is a common situation for spin-stabilized spacecraft. Other Chapters in this Section explore both passive and active attitude stabilization methods.

6.1 Angular Velocity Solutions

6.1.1 *Axisymmetric Inertia Case*

Consider the special case where the spacecraft is axially symmetric. Without loss of generality, let $\hat{\boldsymbol{b}}_3$ be the axis of symmetry. Here $I_1 = I_2 = I_T$ and Eqs. (62) reduce to:

$$I_T\dot{\omega}_1 = -(I_3 - I_T)\omega_2\omega_3 \tag{68a}$$
$$I_T\dot{\omega}_2 = (I_3 - I_T)\omega_3\omega_1 \tag{68b}$$
$$I_3\dot{\omega}_3 = 0 \tag{68c}$$

Eq. (68c) that ω_3 is constant in this case. Differentiating Eqs. (68a) and (68b) and sustituting the results into each yields

$$\ddot{\omega}_1 + \omega_p^2\omega_1 = 0 \tag{69a}$$
$$\ddot{\omega}_2 + \omega_p^2\omega_2 = 0 \tag{69b}$$

with $\omega_p = \left(\frac{I_3}{I_T} - 1\right)\omega_3$. Eqs. (69) are equivalent to spring-mass systems and have the analytical solution:

$$\omega_1(t) = \omega_1(t_0)\cos\omega_p t - \omega_2(t_0)\sin\omega_p t \tag{70a}$$
$$\omega_2(t) = \omega_2(t_0)\cos\omega_p t + \omega_1(t_0)\sin\omega_p t \tag{70b}$$
$$\omega_3(t) = \omega_3(t_0) \tag{70c}$$

6.1.2 *General Inertia Case*

For general rigid body principal inertias Junkins et al. [1973] show that it is possible to write Eqs. (62) as three decoupled second order differential equations

$$\ddot{\omega}_i + A_i\omega_i + B_i\omega_i^3 = 0 \qquad \text{for } i = 1, 2, 3 \tag{71}$$

This homogenous, undamped Duffing equation appears often in structural mechanics problems. However, there the Duffing equation is an approximation the full response. It is amazing that for the rotation motion of a rigid body the angular velocity the Duffing formulation is the *exact differential equation*. The coefficients A_i and B_i are defined in Table 1 where $\Delta_{ij} = I_i - I_j$ and $\kappa_i = 2I_iT - H^2$.

Note that the differential equations in Eq. (71) are uncoupled, they are not independent. The constants A_i depend on the energy T and angular momentum magnitude H. These quantities depend on all three initial conditions of $\omega_i(t_0)$.

Table 1: Rigid Body Duffing Analog Constants

i	A_i	B_i
1	$\dfrac{\Delta_{12}\kappa_3 + \Delta_{13}\kappa_2}{I_1I_2I_3}$	$\dfrac{2\Delta_{12}\Delta_{13}}{I_2I_3}$
2	$\dfrac{\Delta_{23}\kappa_1 + \Delta_{21}\kappa_3}{I_1I_2I_3}$	$\dfrac{2\Delta_{21}\Delta_{23}}{I_2I_3}$
3	$\dfrac{\Delta_{31}\kappa_2 + \Delta_{32}\kappa_1}{I_1I_2I_3}$	$\dfrac{2\Delta_{31}\Delta_{32}}{I_2I_3}$

6.2 Coning Motion

Normally the rotation motion leads to either 2nd order differential equations of attitude coordinates, or two sets of first order differential equations of attitude and angular velocity. For torque-free motion the angular momentum $\boldsymbol{H}$ is inertially constant. This result can be used to reduce the rotational motion to first order differential equations of the attitude coordinates. Using an observation due to Jacobi, the inertial frame is defined such that $\boldsymbol{H} = -H\hat{\boldsymbol{n}}_3$. Using a principal coordinate frame the momentum is written as

$${}^{\mathcal{B}}\boldsymbol{H} = {}^{\mathcal{B}}\begin{pmatrix} I_1\omega_1 \\ I_2\omega_2 \\ I_3\omega_3 \end{pmatrix} = [BN(\psi,\theta,\phi)]\,{}^{\mathcal{N}}\begin{pmatrix} 0 \\ 0 \\ -H \end{pmatrix} \tag{72}$$

As a result of this inertial frame choice, the following coning and precession rates are taken relative to angular momentum vector. Parameterizing the DCM using $(3-2-1)$ Euler angles in Eq. (20) and solving Eq. (72) for $\boldsymbol{\omega}$ yields

$$\begin{pmatrix} \omega_1 \\ \omega_2 \\ \omega_3 \end{pmatrix} = \begin{pmatrix} \frac{H}{I_1}\sin\theta \\ -\frac{H}{I_2}\sin\phi\cos\theta \\ -\frac{H}{I_3}\cos\phi\cos\theta \end{pmatrix} \tag{73}$$

Substituting this $\boldsymbol{\omega}(\theta,\phi)$ result into the $(3-2-1)$ Euler angle differential kinematic equation result in the first order attitude differential equations

$$\dot{\psi} = -H\left(\frac{\sin^2\phi}{I_2} + \frac{\cos^2\phi}{I_3}\right) \tag{74a}$$
$$\dot{\theta} = \frac{H}{2}\left(\frac{1}{I_3} - \frac{1}{I_2}\right)\sin 2\phi\cos\theta \tag{74b}$$
$$\dot{\phi} = H\left(\frac{1}{I_1} - \frac{\sin^2\phi}{I_2} - \frac{\cos^2\phi}{I_3}\right)\sin\theta \tag{74c}$$

Note that the coning rate $\dot{\psi}$ cannot be positive for the general inertia case, while $\dot{\theta}$ and $\dot{\phi}$ can assume either sign. For a axi-symmetric body these attitude rates simplify greatly. Without loss of generality assume that $I_2 = I_3$ and substitute into Eq. (74):

$$\dot{\psi} = -\frac{H}{I_2} \tag{75a}$$
$$\dot{\theta} = 0 \tag{75b}$$
$$\dot{\phi} = H\left(\frac{I_2 - I_1}{I_1I_2}\right)\sin\theta \tag{75c}$$

Note that in this special inertia case all three Euler angle rates have constant rates.

6.3 Polhodes

Let $\boldsymbol{H} = H_1\hat{\boldsymbol{b}}_1 + H_2\hat{\boldsymbol{b}}_2 + H_3\hat{\boldsymbol{b}}_3$ be the angular momentum vector in $\mathcal{B}$ frame components. With torque-free motion the angular momentum magnitude H is constant. Assuming a principal coordinate frame H is written as

$$H^2 = H_1^2 + H_2^2 + H_3^2 = I_1^2\omega_1^2 + I_2^2\omega_2^2 + I_3^2\omega_3^2 \tag{76}$$

In terms of ω_i the momentum constraint describes the surface of an ellipsoid. Using the momentum coordinates H_i the constraint describes the surface of a sphere. Without external torque the power equation in Eq. (59) shows that the energy T is also a constant.

$$T = \frac{1}{2}I_1\omega_1^2 + \frac{1}{2}I_2\omega_2^2 + \frac{1}{2}I_3\omega_3^2 \tag{77}$$

Using $H_i = I_i\omega_i$ the constant energy constrain is written in the energy ellipsoid form:

$$1 = \frac{H_1^2}{2I_1T} + \frac{H_2^2}{2I_2T} + \frac{H_3^2}{2I_3T} \tag{78}$$

Polhodes are three-dimensional line plots of the ω_i evolutions. They are a convenient method to study torque-free rigid body motion. Even with internal friction the angular momentum of a body remains fixed in the absence of external forces. However, the energy can vary. As a result it is common to plot the rigid body motion that result for a fixed H and let the energy levels vary. The momentum constraint in terms of H_i is a sphere in Eq. (76), while the energy constraint in Eq. (78) is an ellipsoid. The actual rotation motion is at the intersection of the momentum sphere and energy ellipsoid.

Without loss of generality, let us assume the inertia ordering $I_1 \geq I_2 \geq I_3$. Figure 4 illustrates the polhodes for the three possible principle axis spin cases. The minimum energy state in Eq. (77) is a pure spin about the maximum principal inertia axis $\hat{\boldsymbol{b}}_1$. The maximum energy state is the spin about the axis of least inertia.

$$T_{\text{max}} = \frac{H^2}{2I_1} \qquad T_{\text{int}} = \frac{H^2}{2I_2} \qquad T_{\text{min}} = \frac{H^2}{2I_3} \tag{79}$$

The T_{max} state represents the smallest energy ellipsoid which still touches the momentum sphere, while T_{min} is the largest ellipsoid to fit inside the sphere and still make contact.

The polhode curves for the energy levels $T_{\text{min}} \leq T \leq T_{\text{max}}$ are illustrated in Figure 5. Small spin departures about the $\hat{\boldsymbol{b}}_1$ and $\hat{\boldsymbol{b}}_3$ axis result in bounded neighboring motion, while any departure from the intermediate axis spin about $\hat{\boldsymbol{b}}_2$ results in unstable motion as predicted be linear stability analysis. Internal friction in a body can reduce the energy level while maintaining a fixed angular momentum vector. The

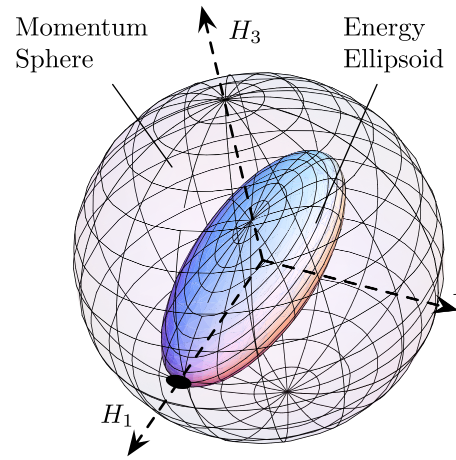

(a) Maximum Inertia Axis Spin (Minimum Energy)

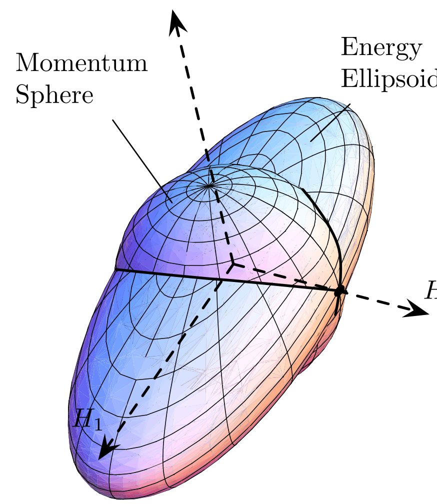

(b) Intermediate Inertia Axis Spin (Intermediate Energy)

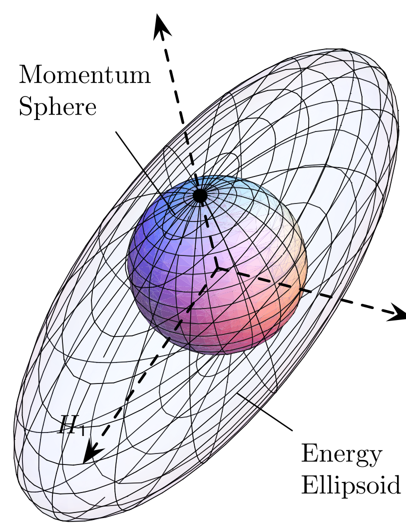

(c) Minimum Inertia Axis Spin (Maximum Energy)

Figure 4: Polhodes of Principal Axis Spin Cases.

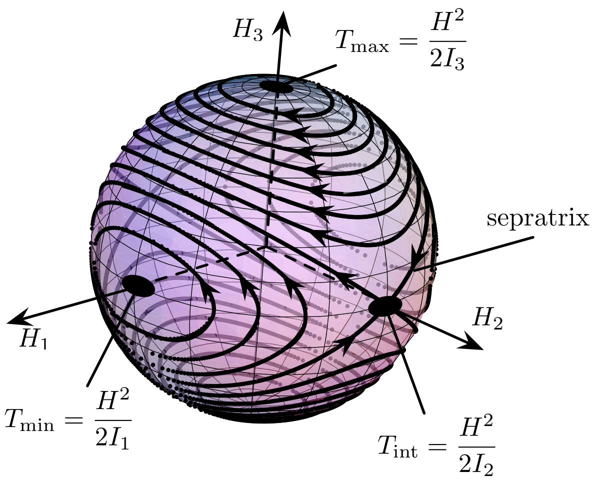

Figure 5: Rigid body Polhode for various energy states

polhodes in Figure 5 illustrate how such an energy loss in a pure min-inertia spin will result in unstable motion because the ω_i eventually intersects with the intermediate axis polhode (septratrix) before settling down to a stable minimum energy spin about the axis of largest inertia.

7 DUAL-SPIN STABILIZATION

While for a single rigid body only the principal axes spin about the axes of largest inertia is passively stable in the presence of energy loss, in many applications (geostationary satellites rotating to point an antenna at a fixed Earth point) it would be of great advantage to be able to stabilize a spacecraft spin about any principal axes, regardless of the corresponding axes inertia. The dual-spin spacecraft is a simple system where passive attitude stability is achieved by adding a single fly-wheel to the rigid spacecraft. Beyond the geostationary communication satellites, another application of the dual-spin concept is the interplanetary Galileo spacecraft which traveled to Jupiter. Here the main antenna needed to continuously point back at the Earth. To stabilize this orientation the half of the body rotated at 3 revolutions per minute, while the sensor components rotated very slowly to align the communication antenna to the slowly changing spacecraft-to-Earth vector. However, this spin rate magnitude must be chosen very carefully. While the dual-spin concept can stabilize any principal axis spacecraft spin, if used incorrectly it can also be the cause of instability.

7.1 Equations of Motion

To develop the dual-spin system equations of motion, without loss of generality, assume that the rotating fly-wheel is aligned with the first principal axis $\hat{\boldsymbol{b}}_1$ of the main spacecraft component as illustrated in Figure 6. Let $\boldsymbol{\omega} = \boldsymbol{\omega}_{\mathcal{B}/\mathcal{N}}$ be

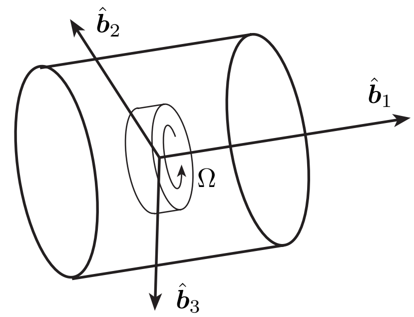

Figure 6: Illustration of a dual-spin spacecraft with the wheel rotation axis aligned with a spacecraft principal axis.

the body angular velocity of the main craft, while $\boldsymbol{\omega}_{\mathcal{W}/\mathcal{B}} = \Omega\hat{\boldsymbol{b}}_1$ is the angular velocity of the fly wheel relative to the spacecraft. The total angular momentum is then given by

$$\boldsymbol{H} = [I_s]\boldsymbol{\omega} + [I_W](\Omega\hat{\boldsymbol{b}}_1 + \boldsymbol{\omega}) \tag{80}$$

where $[I_s]$ is the inertia matrix of the main spacecraft system, while $[I_W]$ is the inertia of the fly wheel component. Note that in the case where the dual-spin craft is rotating an entire segment of the main craft, then $[I_W]$ would be the equivalent spacecraft component inertia matrix. Next, let us define the combined inertia matrix $[I]$ as

$$[I] = [I_s] + [I_W] \tag{81}$$

Assuming a principal coordinate frame $\mathcal{B}$, no external torque vector, and a constant wheel spin rate with $\dot{\Omega} = 0$, we arrive at the three scalar dual-spin spacecraft equations of motion using Euler's equation $\dot{\boldsymbol{H}} = \boldsymbol{0}$:

$$I_1\dot{\omega}_1 = (I_2 - I_3)\omega_2\omega_3 \tag{82a}$$
$$I_2\dot{\omega}_2 = (I_3 - I_1)\omega_1\omega_3 - I_{W_s}\omega_3\Omega \tag{82b}$$
$$I_3\dot{\omega}_3 = (I_1 - I_2)\omega_1\omega_2 + I_{W_s}\omega_2\Omega \tag{82c}$$

Because $\Omega \neq 0$, the only dual-spin equilibrium configuration where $\dot{\boldsymbol{\omega}}$ remains zero is

$$\boldsymbol{\omega}_e = \omega_{e_1}\hat{\boldsymbol{b}}_1 \tag{83}$$

If the wheel spin axis is aligned with another principal body axis, then the dual-spin equilibria would be about this new axis.

7.2 Linear Equilibrium Stability

Next, let us examine the dual-spin spacecraft equilibria stability if the fly wheel is a constantly rotating component, and assuming no system energy loss is present. We linearize the attitude motion about the equilibrium rotation $\boldsymbol{\omega}_e = \omega_{e_1}\hat{\boldsymbol{b}}_1$. Let the actual angular velocity be given by

$$\boldsymbol{\omega} = \boldsymbol{\omega}_e + \delta\boldsymbol{\omega} \tag{84}$$

where $\delta\boldsymbol{\omega} = (\delta\omega_1, \delta\omega_2, \delta\omega_3)^T$ is the departure motion. Substituting this $\boldsymbol{\omega}$ into the equations of motion in Eq. (82) and dropping higher order terms leads to the linearized departure equations of motion:

$$\delta\dot{\omega}_1 = 0 \tag{85a}$$

$$\delta\dot{\omega}_2 = \left(\frac{I_3 - I_1}{I_2}\omega_{e_1} - \frac{I_{W_s}}{I_2}\right)\delta\omega_3 \tag{85b}$$

$$\delta\dot{\omega}_3 = \left(\frac{I_1 - I_2}{I_3}\omega_{e_1} + \frac{I_{W_s}}{I_3}\right)\delta\omega_2 \tag{85c}$$

Note that because $\delta\dot{\omega}_1 = 0$, the departure angular velocity about $\hat{\boldsymbol{b}}_1$ (i.e. the fly wheel spin axis in this case), is only marginally stable with $\omega_1(t) = \omega_{e_1} + \delta\omega_1(t_0)$ being constant.

To determine the stability of the $\delta\omega_2(t)$ and $\delta\omega_3(t)$ motions, we differentiate Eq. (85b) and substitute Eq. (85c) to find

$$\delta\ddot{\omega}_2 + k\delta\omega = 0 \tag{86}$$

where the stiffness-like parameter k is

$$k = \frac{\omega_{e_1}^2}{I_2 I_3}\left(I_1 - I_3 + I_{W_s}\hat{\Omega}\right)\left(I_1 - I_2 + I_{W_s}\hat{\Omega}\right) \tag{87}$$

and $\hat{\Omega} = \frac{\Omega}{\omega_{e_1}}$ is the non-dimensional fly-wheel spin rate. For the non-spin axis departure velocities to be stable we require

$$k > 0 \tag{88}$$

Given the principal inertias I_1, I_2 and I_3, we would like to determine for what range of values $\hat{\Omega}$ the dual-spin spacecraft motion is passively stable. There are two critical wheel speeds which cause the inequality conditions to be either true or false:

$$\hat{\Omega}_1 = \frac{I_3 - I_1}{I_{W_s}} \tag{89a}$$

$$\hat{\Omega}_2 = \frac{I_2 - I_1}{I_{W_s}} \tag{89b}$$

The dual-spin stability condition in Eq. (88) is satisfied if:

$$\text{Condition 1:} \quad \hat{\Omega} > \hat{\Omega}_1 \quad \text{and} \quad \hat{\Omega} > \hat{\Omega}_2 \tag{90a}$$

$$\text{Condition 2:} \quad \hat{\Omega} < \hat{\Omega}_1 \quad \text{and} \quad \hat{\Omega} < \hat{\Omega}_2 \tag{90b}$$

Let us examine these 2 stability conditions for three types of principal axis rotations. First, consider the maximum inertia spin scenario where $I_1 > I_2 > I_3$. Because I_1 is the largest inertia, both $\hat{\Omega}_1$ and $\hat{\Omega}_2$ are negative values with $\hat{\Omega}_1 < \hat{\Omega}_2$. The resulting ranges of stabilizing $\hat{\Omega}$ values are graphically illustrated in Figure 7(a). Note that because the maximum inertia spin is stable in absence of the fly wheel, the feasible $\hat{\Omega}$ range must include the origin.

The stabilizing fly wheel spin rates for the case where the spacecraft is to rotate about an intermediate axis of inertia is illustrated in Figure 7(b). As expected, note that here the origin is not included in the stabilizing $\hat{\Omega}$ range. Without the stabilizing effect of the fly wheel, the single rigid body spin about the intermediate axis of inertia is unstable.

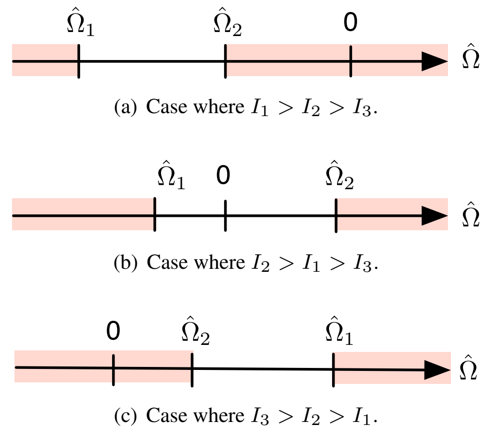

(a) Case where $I_1 > I_2 > I_3$.

(b) Case where $I_2 > I_1 > I_3$.

(c) Case where $I_3 > I_2 > I_1$.

Figure 7: Stabilizing $\hat{\Omega}$ range (shaded) illustration.

Lastly, we explore the stabilizing wheel speed range for a minimum axis of inertia spin where $I_3 > I_2 > I_1$. The admissible wheel speeds are illustrated in Figure 7(c). Because the minimum inertia spin case is linearly stable in the absence of a fly wheel, the origin is once again included in the admissible range. However, there is still finite range of positive $\hat{\Omega}$ values which would lead to an unstable system.

If the system undergoes energy loss (wheel bearing friction), then the above stability analysis must be modified. Dual-spin spacecraft stability analysis with energy loss is discussed in further detail in both Hughes [1986] or Curtis [2010].

8 EXTERNAL TORQUES FOR PASSIVE CONTROL

Next, let us consider what external torques can be used to passively stabilize a spacecraft without resorting to a feedback control strategy.

8.1 Gravity Gradient Torques

Not all parts of a rigid body will experience the same gravitational attraction to the planet they are orbiting due to differing separation distances. While position difference are very small, they due lead to a noticeable net torque being applied to the spacecraft called gravity gradient torque.

Assume the center of mass of object $\mathcal{B}$ Earth's center is the inertial position vector $\boldsymbol{R}_c$. Let the vector $\boldsymbol{L}_G$ be the external gravity gradient torque experienced by a rigid object measured about its center of mass. For a solid body this torque is defined through

$$\boldsymbol{L}_G = \int_{\mathcal{B}} \boldsymbol{r} \times \mathrm{d}\boldsymbol{F}_G \tag{91}$$

where the vector $\boldsymbol{r}$ is the position vector of an infinitesimal body element relative to the center of mass and $\boldsymbol{F}_G$ is the gravitational attraction experienced by this element. Using Newton's Gravitational Law this force is written as

$$\mathrm{d}\boldsymbol{F}_G = -\frac{GM_e}{|\boldsymbol{R}|^3}\boldsymbol{R}\mathrm{d}m \tag{92}$$

where M_e is Earth's mass, $\mathrm{d}m$ is the body element mass and $\boldsymbol{R}$ is its inertial position vector measured from Earth's center.

$$\boldsymbol{R} = \boldsymbol{R}_c + \boldsymbol{r} \tag{93}$$

Substituting Eq. (92) into the $\boldsymbol{L}_G$ expression, and expanding use a binomial expansion to first order, yields the general gravity gradient torque expression: ([Junkins and Turner, 1986, Greenwood, 1988, Schaub and Junkins, 2010])

$$\boldsymbol{L}_G = \frac{3GM_e}{R_c^5}[\tilde{\boldsymbol{R}}_c][I]\boldsymbol{R}_c \tag{94}$$

Note that no particular frame has been chosen in Eq. (94) to express this torque. For example, if orbit frame $\mathcal{O}$: $\{\hat{\boldsymbol{o}}_\theta, \hat{o}_h, \hat{\boldsymbol{o}}_r\}$ vector components are chosen, the ${}^{\mathcal{O}}\boldsymbol{R}_c = [0, 0, R_c]^T$ and ${}^{\mathcal{O}}[I]$ is a fully populated matrix for general spacecraft orientations. Here the gravity gradient torque expression in Eq. (94) reduces to:[Schaub and Junkins, 2010]

$${}^{\mathcal{O}}\boldsymbol{L}_G = \frac{3GM_e}{R_c^3}(-I_{23}\hat{\boldsymbol{o}}_r + I_{13}\hat{\boldsymbol{o}}_h) \tag{95}$$

Note that the gravity gradient torque will never produce a torque about the orbit radial axis. In contrast, assume $\mathcal{B}$ is a principal body frame. Here ${}^{\mathcal{B}}\boldsymbol{R}_c = [R_{c_1}, R_{c_2}, R_{c_3}]^T$ and ${}^{\mathcal{B}}[I] = \mathrm{diag}(I_1, I_2, I_3)$, leading to the simple expression:

$$\boldsymbol{L}_G = \frac{3GM_e}{R_c^5} {}^{\mathcal{B}}\!\begin{pmatrix} R_{c_2}R_{c_3}\,(I_{33} - I_{22}) \\ R_{c_1}R_{c_3}\,(I_{11} - I_{33}) \\ R_{c_1}R_{c_2}\,(I_{22} - I_{11}) \end{pmatrix} \tag{96}$$

Studying Eq. (96) it is clear that the gravity gradient torque can be zero for several scenarios. For example, if the spacecraft body shape is such that $I_1 = I_2 = I_3$ (spherical symmetry for example) leads to a zero torque. Further, if $\boldsymbol{R}_c$ is aligned with one of the principal body axes, then one R_{c_i} vector component is non-zero, while the remaining two are zero. Here too the torque $\boldsymbol{L}_G$ is zero.

To determine all possible gravity gradient equilibrium orientations, one of the body fixed axes must align with the orbit nadir axis $\hat{\boldsymbol{o}}_r$. To ensure that $\dot{\boldsymbol{\omega}}$ (equilibrium condition), the gyroscopic term $[\tilde{\boldsymbol{\omega}}][I]\boldsymbol{\omega}$ in Eq. (61) requires that the other two body axes are aligned with either the along-track direction $\hat{\boldsymbol{o}}_\theta$ or the orbit normal direction $\hat{\boldsymbol{o}}_h$. Thus, a spacecraft is in a gravity gradient equilibrium orientation if the orbit frame axes are also principal axes of the body inertia matrix $[I]$.

To analyze the stability of the spacecraft attitude motion about, let us assume small angular departures (linearized stability analysis), and use the $3-2-1$ Euler angles (ψ, θ, ϕ) to describe the departure orientations. Assuming a circular orbit with a mean orbit rate Ω, the linearized pitch equation becomes:

$$\ddot{\theta} + 3\Omega^2\left(\frac{I_{11} - I_{33}}{I_{22}}\right)\theta = 0 \tag{97}$$

where I_{11} is the principal inertia about the $\hat{\boldsymbol{o}}_{theta}$ orbit along-track axis, I_{22} is the principal inertia about $\hat{\boldsymbol{o}}_h$, and I_{33} is the principal inertia about the orbit radial axis $\hat{\boldsymbol{o}}_r$. These pitch equations are the dynamical equivalent of a simple spring-mass system. It is immediately clear from linear control theory that for the pitch mode to be stable

$$I_{11} \geq I_{33} \tag{98}$$

must be true. Thus, for pitch stability, the spacecraft orientation must be chosen such that the inertia about the along-track axis must be larger than the inertia about the orbit radial axis.

The linearized roll and yaw motions are given through the coupled equations:

$$\begin{pmatrix}\ddot{\phi} \\ \ddot{\psi}\end{pmatrix} + \begin{bmatrix} 0 & \Omega\,(1 - k_Y) \\ \Omega\,(k_R - 1) & 0 \end{bmatrix}\begin{pmatrix}\dot{\phi} \\ \dot{\psi}\end{pmatrix} + \begin{bmatrix} 4\Omega^2 k_Y & 0 \\ 0 & \Omega^2 k_R \end{bmatrix}\begin{pmatrix}\phi \\ \psi\end{pmatrix} = 0 \tag{99}$$

where the inertia ratios k_R and k_Y are defined as

$$k_R = \frac{I_{22} - I_{11}}{I_{33}} \tag{100}$$

$$k_Y = \frac{I_{22} - I_{33}}{I_{11}} \tag{101}$$

To guarantee stability it is necessary and sufficient that

$$1 + 3k_Y + k_Y k_R > 4\sqrt{k_Y k_R} \tag{102}$$

$$k_R k_Y > 0 \tag{103}$$

The two possible regions where we have marginal stability on all three degrees of freedom are illustrated in Figure 8. Region I requires that

$$I_{22} \geq I_{11} \geq I_{33} \tag{104}$$

This gravity gradient stabilized configuration requires that the inertia about the orbit normal axis $\hat{\boldsymbol{o}}_h$ is the largest inertia. The configurations in Region II are not typically employed because they are unstable if damping and energy loss is considered.

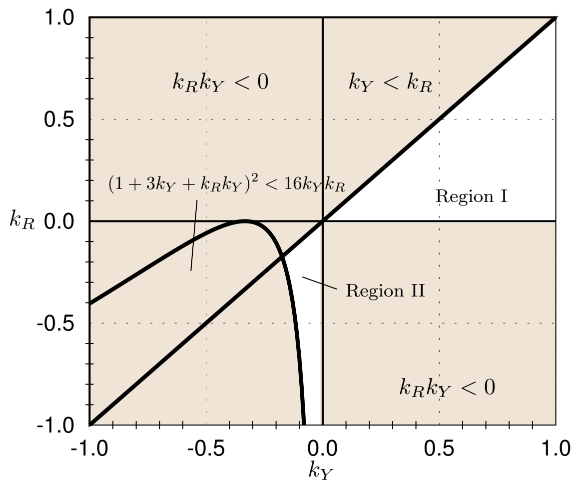

Figure 8: Linearized Gravity Gradient Spacecraft Stability Regions

8.2 Atmospheric Torques

In the rarefied atmosphere of low Earth orbits, a small amount of gas molecules can hit the spacecraft and impart a force. Because the local gas dynamics behaves like a free molecular flow, the deflected gas particles have a negligible influence on the gas particles. This non-interaction of incoming and deflected gas particles allows the net aerodynamic force or torque to be computed by summing the contributions of each of the spacecraft components individually. This allows the vehicle shape to be dissected into simple sub-shapes to easy the aerodynamic force and torque computation.

A conservative estimate of the total aerodynamic force F_a acting on the spacecraft can be obtained through the following approximation:

$$F_a = \frac{1}{2} C_D \rho v^2 A \tag{105}$$

where ρ is the local atmospheric density, A is the projected area of the spacecraft normal to the incident flow (spacecraft velocity direction), v is the velocity of the spacecraft relative to the local atmosphere, and C_D is the drag coefficient. To obtain a conservative estimate of the atmospheric force, a conservative value of C_D should be used.

The magnitude of the atmospheric torque is estimated using

$$L_a = l F_a \tag{106}$$

where is the moment arm of the center of pressure relative to the spacecraft center of mass. For conservative estimates, this moment arm is assumed to be at least one-third of the spacecraft's maximum dimension. This includes all appendages, and should be done even if the spacecraft is symmetric.

Equilibrium orientations subject to the atmospheric torque are such orientations where L_a is zero. This can be achieved by having symmetrical atmospheric pressure distribution relative to the spacecraft velocity vector. Such symmetry will cause the atmospheric torque about the spacecraft components to mutually cancel, even though a net atmospheric force (atmospheric drag) is applied.

Another particular attitude is the Torque Equilibrium Attitude (TEA). This orientation ensures that all external torques acting on the craft mutually cancel each other. For example, if the spacecraft shape causes a small atmospheric torque which cause the craft to begin to rotate, it is possible to orient the craft such that the gravity gradient torque perfectly cancels the atmospheric torque. For example, the space station often flies in TEA's to avoid having external torques cause excessive momentum build-up.

8.3 Magnetic Torques

If the spacecraft contains a magnetic field due to the presence of magnetic torque rods, then these can also produce an external torque $\boldsymbol{L}_m$ due to the interaction with Earth's magnetic field. If $\boldsymbol{m}$ is the magnetic moment of the spacecraft, and $\boldsymbol{B}$ is the geocentric magnetic flux density, the resulting magnetic torque is given by[Wertz and Larson, 1999]

$$\boldsymbol{L}_m = \boldsymbol{m} \times \boldsymbol{B} \tag{107}$$

For a spinning spacecraft motion the induced eddy currents can cause a small magnetic torque. Such torques [Wertz and Larson, 1999] can cause the spin axis to precess, and also result in nutation damping.

9 CONCLUSION

This Chapter develops the fundamental kinematics and kinetics of a single rigid body. The orientation of the body is tracked by studying the rotation of a body-fixed coordinate frame $\mathcal{B}$. Analytical solutions to the body angular velocities are explored for the axi-symmetric and general inertia case. Assuming no external torque, the linear spacecraft spin stability about the principal inertia axis is explored. Using polhode plots, the torque free response is illustrated for a range of spin conditions, including the case where the body is losing energy due to internal damping. Passive attitude stability can be achieved using dual-spin configurations, or external influences such as the gravity gradient of atmospheric torques. The following Chapters explore the attitude response of a spacecraft using active control methods (applying external torques through thrusters or using internal momentum exchange devices), as well as how to estimate the orientation parameters using both external observations (sun or star sensor) and internal rate measurements.

REFERENCES

Curtis HD. *Orbital Mechanics for Engineering Students*. 2nd Edition, Elsevier Aerospace Engineering Series, Burlington, MA, 2010.

Greenwood DT *Principles of Dynamics*. Prentice-Hall, Inc, Englewood Cliffs, New Jersey, 2nd edition, 1988.

Hughes PC. *Spacecraft Attitude Dynamics*. John Wiley & Sons, Inc., New York, 1986.

Junkins JL, Jacobson ID, and Blanton JN. a nonlinear oscillator analog of rigid body dynamics. *Celestial Mechanics and Dynamical Astronomy*, Vol. 7, No. 4, 1973, pp. 398–407.

Junkins JL and Turner JD. *Optimal Spacecraft Rotational Maneuvers*. Elsevier Science Publishers, Amsterdam, Netherlands, 1986.

Likinsj PW. *Elements of Engineering Mechanics*. McGraw-Hill, New York, 1973.

Schaub H and Junkins JL. Stereographic orientation parameters for attitude dynamics: A generalization of the rodrigues parameters. *Journal of the Astronautical Sciences*, Vol. 44, No. 1, 1996, pp. 1–19.

Schaub H and Junkins JL. *Analytical Mechanics of Space Systems*. 2nd Edition, AIAA Education Series, Reston, VA, 2009.

Sheppard SW. Quaternion from rotation matrix. *AIAA Journal of Guidance, Control, and Dynamics*, Vol. 1, No. 3, 1978, pp. 223–224.

Shuster MD. A survey of attitude representations. *Journal of the Astronautical Sciences*, Vol. 41, No. 4, 1993, pp. 439–517.

Sidi MJ. *Spacecraft Dynamics and Control: A Practical Engineering Approach*. Cambridge University Press, Cambridge, England, 1997.

Thomson WT. *Introduction to Space Dynamics*. Dover Publications, Toronto, Canada, 1986.

Tsiotras P and Longuski JM. A new parameterization of the attitude kinematics. *Journal of the Astronautical Sciences*, Vol. 43, No. 3, 1996, pp. 342–262.

Wertz, JR and Larson WJ. *Space Mission Analysis and Design* Microcosm, Inc., El Segundo, CA, 3rd edition, 1999.

Whittaker ET. *Analytical Dynamics of Particles and Rigid Bodies*. Cambridge University Press, 1965 reprint. pp. 2–16.

Wie B. *Space Vehicle Dynamics and Control*. AIAA Education Series, Reston, VA, 2nd edition, 2008.

Wiener TF. *Theoretical Analysis of Gimballess Inertial Reference Equipment Using Delta-Modulated Instruments*. Ph.D. dissertation, Department of Aeronautics and Astronautics, Massachusetts Institute of Technology, March 1962.

Wiesel WE. *Spaceflight Dynamics*. McGraw-Hill, Inc., New York, 1989.